Article

Nuclear Analysis of High-Power LIEBE Molten Target at CERN for the Production of Radioisotopes

Benjaminas Togobickij, Mantas Povilaitis, Andrius Slavickas, Thierry Stora, Vincent Barozier and Gediminas Stankūnas

Special Issue

Selected Papers from the 18th International Conference of Young Scientists on Energy and Natural Sciences Issues (CYSENI 2022)

Edited by
Dr. Sigitas Rimkevičius and Dr. Rolandas Urbonas

Article

Nuclear Analysis of High-Power LIEBE Molten Target at CERN for the Production of Radioisotopes

Benjaminas Togobickij [1,*], Mantas Povilaitis [1], Andrius Slavickas [1], Thierry Stora [2], Vincent Barozier [2] and Gediminas Stankūnas [1]

1 Laboratory of Nuclear Installation Safety, Lithuanian Energy Institute, LT-44403 Kaunas, Lithuania
2 European Organization for Nuclear Research (CERN), 1211 Geneva, Switzerland
* Correspondence: benjaminas.togobickij@lei.lt

Abstract: To enhance the production of short-lived isotopes, higher beam powers are sought, which require targets able to accommodate them. One such target prototype is a liquid metal target LIEBE, developed at CERN. In this paper, a simulation of the proton beam interaction with the LIEBE target is presented. Simulations were performed by a series of proton transport calculations using the MCNP Monte Carlo code. The latest LIEBE target MCNP input was created in high-fidelity geometry, and the FENDL-3.1 cross-section data library was used. Flux and dose rate maps in the LIEBE target obtained from the simulations are presented in the paper. The maximum obtained dose around the target is roughly 361 Sv/h for gamma rays and 214 Sv/h for neutrons. The 70 MeV–100 µA proton beam penetrates roughly 7 mm deep into the liquid eutectic lead–bismuth. Based on this, further required changes to the LIEBE target can be evaluated.

Keywords: Monte Carlo; LIEBE; MCNP; dose rates

1. Introduction

Radioactive isotopes are extensively used in medicine, industry and research. Isotope Separator Online (ISOL) facilities linked to particle accelerators are commonly used to efficiently produce radioactive isotopes in the form of Radioactive Ion Beams (RIBs). In ISOL facilities, RIBs are created by the beam interaction with a target, resulting in radioisotope production. However, increasing demand for larger amounts and more exotic radioisotopes for both research and medical applications is becoming challenging to meet for beam and target configurations of current ISOL facilities.

To enhance the production of short-lived isotopes higher primary beam intensities are sought in the next generation of radioactive ion beam installations. However, current targets are unable to accommodate high-power beams. The design of high-power targets is complicated regarding the ability to maintain a uniform temperature profile in the target and a reasonable lifetime. Another challenge at high beam powers is adequate heat removal from the target [1].

The European Organization for Nuclear Research, known as CERN, operates an ISOL facility called ISOLDE (acronym for Isotope Separator Online DEvice). It directs a high-intensity proton beam from the Proton Synchrotron Booster onto specially developed thick targets. Additionally, there is a second target placed behind ISOLDEs, in CERNs MEDICIS (an acronym for Medical Isotopes Collected from ISOLDE) facility, which is focused on medical radioisotopes. Radioisotopes produced at the MEDICIS facility are extracted via mass separation, implanted in a small foil and delivered to other research facilities. In this context, a high-power target for testing in the ISOLDE facility was developed. It was proposed for short-lived isotopes by the European Isotope Separation Online (EURISOL) project. The proposed design resulted in a liquid high-power target concept instead of the currently mainly used solid targets. To operate a liquid target at high power, its concept

was based not on the currently common static-bath design, but on a liquid metal loop. When using a liquid metal loop, beam irradiation, heat removal and isotope diffusion are functionally decoupled from each other. High heat removal rates can be achieved through the circulation of the liquid target material and the use of a heat exchanger.

To validate this concept, a target prototype called LIEBE (Liquid Eutectic Lead Bismuth Loop Target for EURISOL) was designed and assembled [2]. A new target development requires several different investigations. Among them isevaluation of radiological conditions during the operation of LIEBE target. To estimate arising neutron and gamma radiation fluxes, studies of the proton beam interaction with the LIEBE target are needed. However, since LIEBE is a new target, there are only a few publications dedicated to proton beam–LIEBE interaction and the resulting radiological conditions.

Design studies were published in M. Delonca Ph.D. thesis [3]. They are dedicated to the functioning of the target; for example, radioisotope yield, thermal–hydraulic parameters, LBE droplet formation, etc. There are later simulations published of proton beam–LIEBE target interaction used to evaluated energy deposition in the irradiation chamber around the proton beam path using FLUKA code [4]. However, these calculations were focused on deposited energy, since their aim was to study the thermohydraulic response of the target. Monte Carlo code calculations, including isotope generation in the LIEBE target, were performed later using ABRALA and FLUKA codes by F. Boix Pamies et al. [1]. The production rate of tin isotopes in the vicinity of ^{100}Sn with future beam parameters of 2 GeV and 4 µA were calculated. However, these simulations were conducted for hypothetical, lanthanum-based, and not the lead–bismuth-based eutectic.

To compliment the literature and provide new knowledge regarding the LIEBE target interaction with proton beam, this paper presents a numerical study of the interaction and resulting neutron and gamma radiation. Presented simulations were performed by a series of proton transport calculations using the Monte Carlo N-Particle (MCNP) code [5]. The latest LIEBE target model was created in high-fidelity geometry and FENDL-3.1 (Fusion Evaluated Nuclear Data Library) cross-section data library was used. Simulations produced neutron and gamma fluxes and dose rate maps of the operating LIEBE target.

The paper is organized as follows: Section 2 explains the general methodology of MCNP code. In the Section 3, the process of converting the LIEBE CAD model, provided by CERN, to an MCNP input is described. In Section 4, obtained results of the proton transport calculations and the distribution of neutron and gamma dose rates are presented and discussed.

2. MCNP Code

The MCNP code was used to simulate the proton beam's interaction with the target and generated neutron and gamma transport. In neutron and gamma transport simulations, typical output is neutron and gamma fluxes. To estimate the cell flux, the track length, collision, absorption and point flux substitution methods are used [6].

The particle fluence over a cell volume in MCNP is defined by the formula:

$$\Phi(V) = \frac{1}{V} \int_V dV \int_E dE \int_{4\pi} d\Omega \Phi(r, E, \Omega), \tag{1}$$

where V is the volume of the cell, E is the energy of the particle at the volume and $\Phi(r, E, \Omega)$ is the energy and angular distribution of the fluence as a function of position, which can be expressed as the sum of the contributions of each scattering [7].

It is also necessary to find an estimate of the standard deviation of the mean of the results μ and the relative error of the particle histories. The standard deviation of the mean in MCNP is calculated as follows:

$$\sigma_\mu = \frac{\sigma}{\sqrt{N}}, \tag{2}$$

where σ—standard deviation of history results, N—number of particles per source particles.

To reduce the standard deviation σ_μ, it is required to decrease the variance of the histories or increase the number of histories [8]. Since the model is very detailed, to obtain statistically acceptable results, a longer computing time is needed to increase the number of particle histories. However, for high-fidelity mesh calculations, the relative standard deviation is less suitable for obtaining a convincing estimate of the relative error. The relative error is usually calculated as follows:

$$R = \frac{\sigma_\mu}{\mu}. \tag{3}$$

MCNP can provide information on the reliability of results using ten statistical tests, and if any of the ten tests fails, MCNP will produce additional outputs about the failed tests [7]. This paper considers the neutron and gamma-induced dose rates around the LIEBE target. The dose rate estimation can be obtained after the neutron and gamma flux calculations using the Formula [9]:

$$H = \sum \Phi(V)h, \tag{4}$$

where h is the fluence-to-dose conversion coefficient.

3. LIEBE Target Model and Conversion

At present, LIEBE is a prototype liquid metal ion beam target (see Figure 1) aimed at solving issues of accommodating a high-power beam and ensuring adequate extraction of short-lived radioisotopes [2]. Liquid target material circulates through different functional components of the target–irradiation chamber, diffuser and heat exchanger. LIEBE uses a lead–bismuth eutectic (LBE) circulating in a 200 °C–600 °C temperature loop. The eutectic is driven by an electromagnetic pump to an irradiation chamber, where it is subjected to the high-power proton beam.
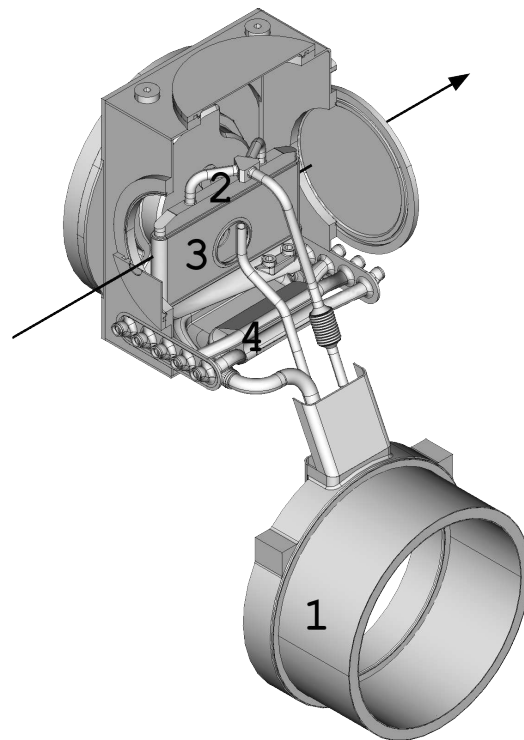

Figure 1. CAD model of the LIEBE target (1—electromagnetic pump, 2—irradiation chamber, 3—diffusion chamber, 4—heat-exchanger, the arrow shows the beam direction).

The irradiation chamber has a length of 210 mm and a width of 10 mm. The proton beam enters the chamber through the half-cylinder-shaped window. Chamber itself is

separated into three parts by two internal feeder grids. These two intermediate grids are devised to improve profiles of LBE flow velocities. They should develop a more uniform flow evacuation–velocity distribution at the chamber exit.

Irradiated eutectic then falls through a grid separating irradiation and diffusion chambers. This grid is intended for the shower formation—it should fragment falling LBE into 0.4 mm diameter droplets, which would then fall along the height of the diffusion chamber. The diffusion chamber is designed to accommodate the fast extraction of radioisotopes from falling metal droplets. Such a design is needed to enable the extraction time of short-lived isotopes faster than their half-lives.

A high-power proton beam will deposit a large amount of excess heat to the circulating eutectic. To remove the excess heat, eutectic will flow to the water-cooled heat exchanger from the diffusion chamber. The LIEBE device, presented in Figure 1 is encapsulated inside a container with an argon atmosphere, to prevent air exposition and oxidation of the liquid LBE [3].

The first milestone of the study was the creation of a calculation model. To achieve this, a recent CAD model of the LIEBE target was used. Therefore, the production of the MCNP input file required the conversion of the CAD model to a 3D description of the MCNP geometry. This was achieved in the SALOME environment [10] using the McCAD [11] conversion tool, which is a Monte Carlo CAD-based modeling program used to convert CAD drawings to the geometries of MCNP, TRIPOLI [12] and Geant4 [13] codes. With the help of the code, the available CAD model was decomposed, i.e., divided by all geometry surfaces and converted to MCNP format. Due to the complex and detailed nature of the existing CAD model, automated conversion was hardly possible, requiring individual manual modification of many components.

The conversion process involved several challenges. These are caused by the fact that certain parts of the CAD model do not have an MCNP counterpart in the geometry description. In Figure 2, the detected problem areas of the CAD model are presented, i.e. spline (surfaces defined by control points) and torus surfaces whose axes of revolution are not perpendicular to any of the x, y or z axes. The problematic areas had to be converted into basic surfaces: cylinders, planes and perpendicular to x, y and z planes tori. The conversion was achieved using the SALOME software McCAD module.
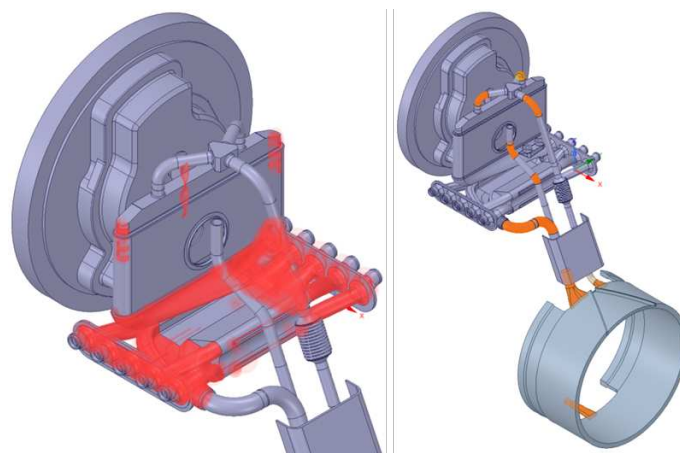

Figure 2. Problematic areas (red and orange colors) of LIEBE target CAD model.

Since the CAD model of the LIEBE target was complex and detailed, many elements of the model also needed to be manually simplified. These modifications were primarily spline and torus surface approximations with cylinders and planes (as in Figure 3).
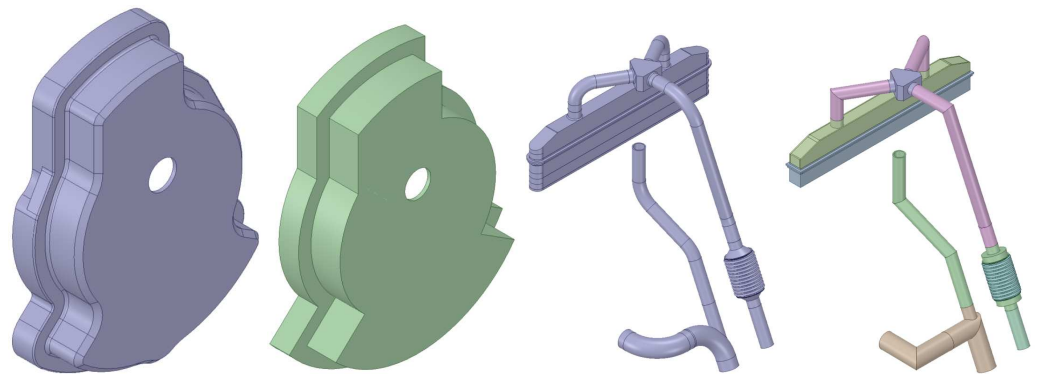
Figure 3. Examples of the LIEBE target approximation.

The most complex LIEBE component was the heat exchanger and its component tubes (see Figure 4), which was approximated by a rectangular prism of a water–steel mixture.
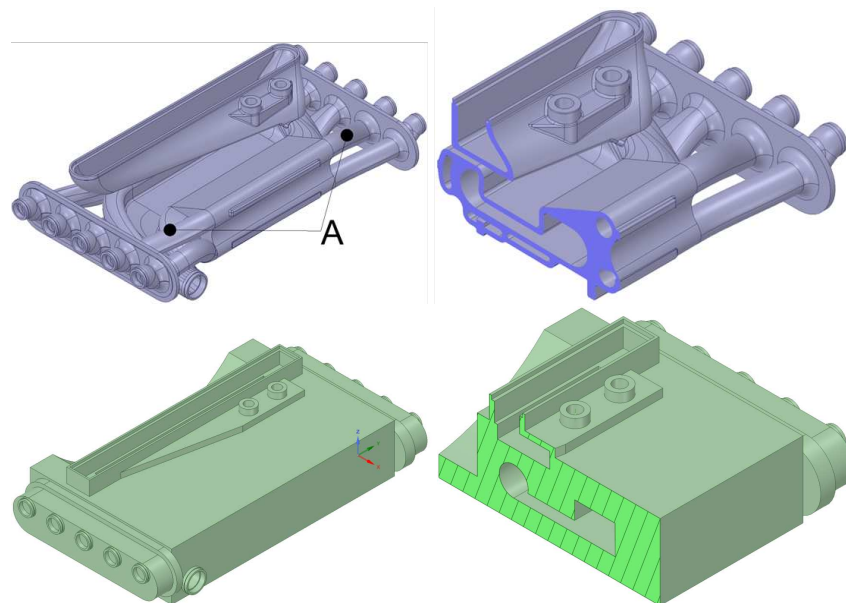

Figure 4. The LIEBE target heat-exchanger approximation (CAD model—top, an approximation –bottom, A—heat-exchanger tubes).

Not much less complex was the LBE loop, which is shown in Figure 5. A fragment of the approximation is presented in the same figure on the right side in green.

As the conversion process continued, it was noticed that the McCAD software was not accurately converting cone-shaped surfaces, so they also had to be approximated using the methods described above (replacing the cone with a cylinder or connecting cylinders of different radii). More details are given in Figure 5 (bottom), where the original representation of the lead outline from the CAD model is shown on the left, and the approximation made by replacing the cone and spline surfaces with cylinders and planes is shown on the right.

Other components of the LIEBE target, such as the vessel and container, were approximated using analogous methods.

In the analyzed CAD LIEBE target model, parts that had mutual intersections were detected. Such parts of the model were individually modified. Intersections in the irradiation chamber were resolved by dividing the parts into separate segments, while some other intersections were eliminated by reducing the lengths of the cylinders.
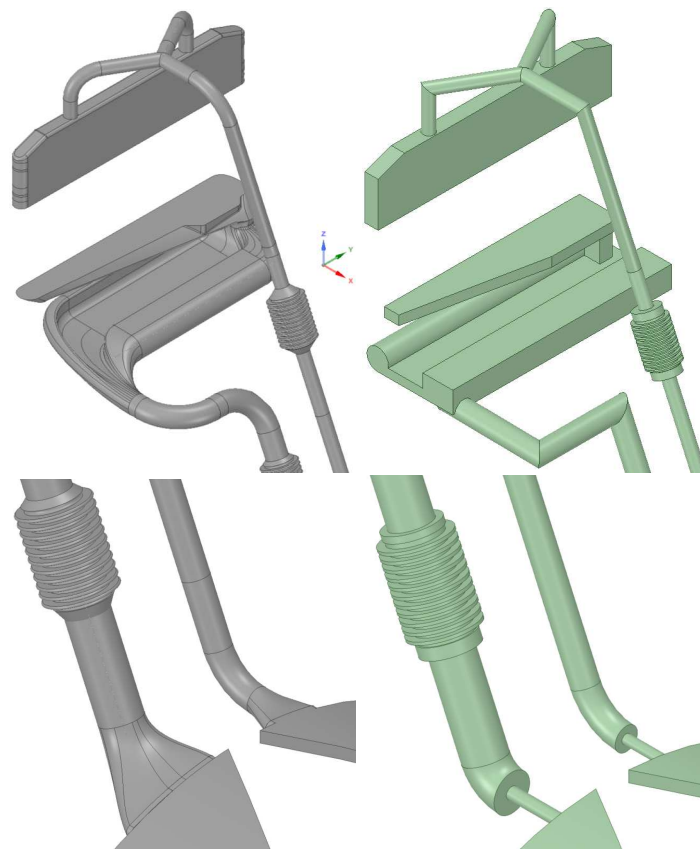
Figure 5. LBE approximation (CAD model— gray, an approximation—green).

Detailed analysis of the CAD model and predicted physical processes and possible nuclear reactions during the beam-target collision allowed us to simplify the CAD model by discarding certain parts, which were eliminated because their inclusion makes the model geometrically complex, significantly impacting the calculation time, but not to their results.

The next stage of model conversion is model decomposition. The McCAD 0.5.1 software package performs the decomposition correctly for simple components, but it fails for more complex components. For this reason, the model had to be manually decomposed. Decomposition was performed using methods aimed at minimizing the number of parts to be decomposed (see Figure 6 for more details). Analogously, all components of the CAD model of the LIEBE target were decomposed.

During the final stage of converting the CAD model, it became clear that additional challenges were caused by the specificity of SALOME, which divides the surface of a torus and a cylinder into two parts, so such surfaces were combined manually using the geometry module in the SALOME environment.

Since all components of the target model were separately decomposed, after combining all the decomposition parts into homogeneous components in the SALOME environment, geometric parts were obtained that formed different cells in the MCNP input file. The described cells of the components whose automatic conversion did not give the desired result or were wrongly converted were corrected in the MCNP environment (see Figure 7).
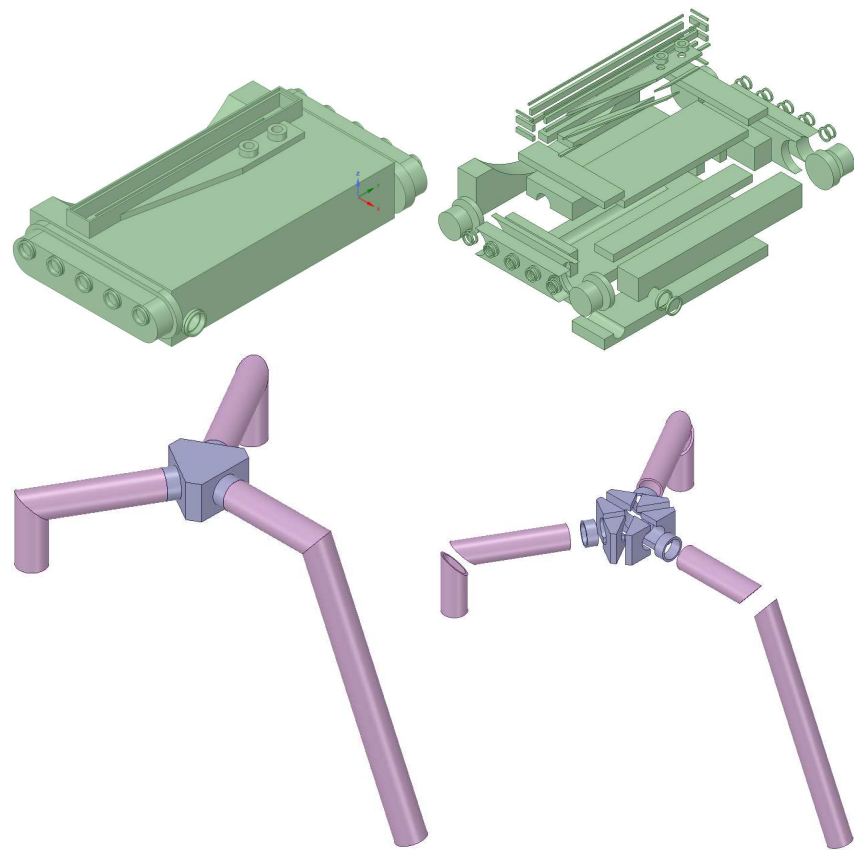
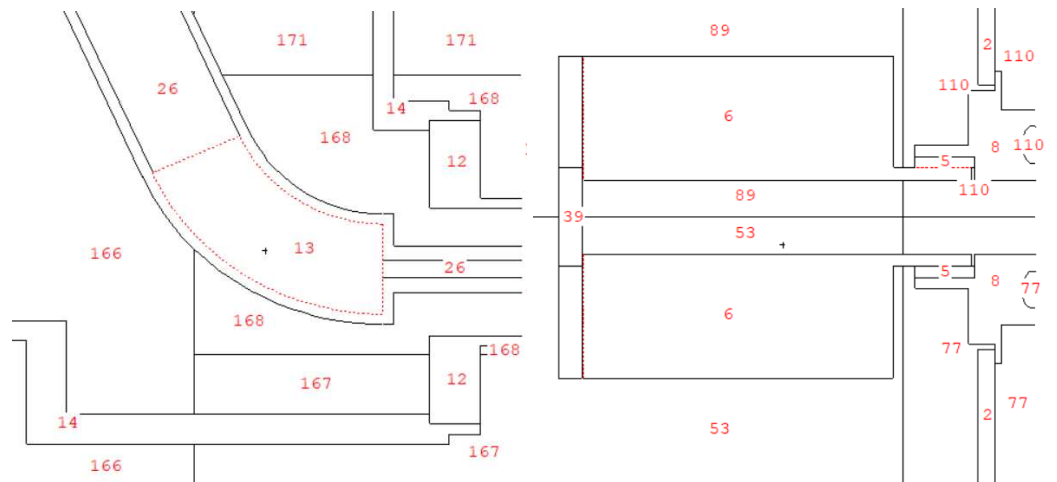**Figure 6.** Example of the LIEBE target decomposition.

Figure 7. Examples of incorrectly converted and later corrected cells in the MCNP environment (red dotted lines denote incorrectly defined cells).

Every geometry conversion from one system to another creates a series of problems and challenges. This case did not turn out to be exceptional, so the detailed sequence of steps presented in this paragraph and the work in this area allowed the conversion to be carried out with precision in terms of geometry. Figure 8, presenting a comparison between the converted model and original CAD model cross sections from Figure 9, shows that the MCNP model was created in such a way that it retained the majority of the detail from the original LIEBE CAD model. Such conversion was performed for the first time for the LIEBE target.
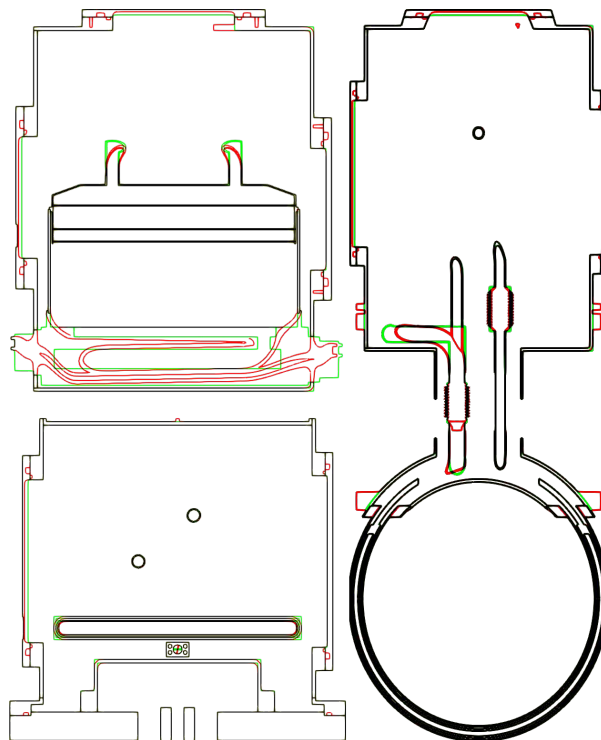
Figure 8. A comparison between the original LIEBE CAD model and the converted MCNP model cross sections. Red lines are of the original LIEBE cad model, green lines are of the converted MCNP model and black lines are the intersections of these lines.
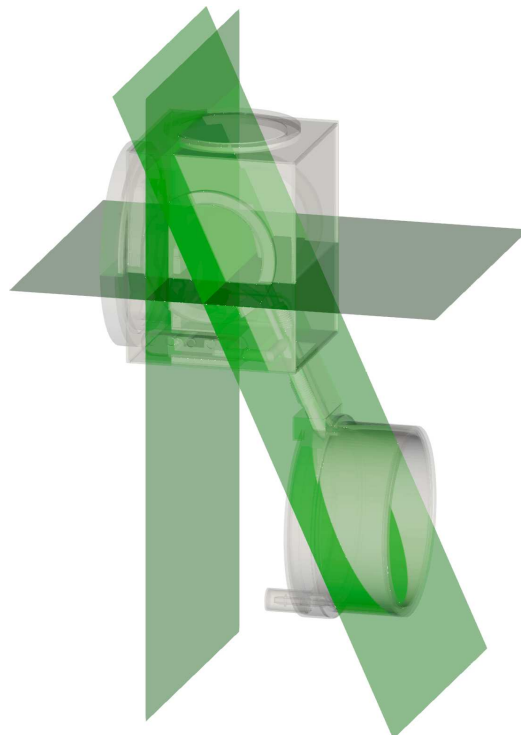

Figure 9. Different cross-section planes used for the figures throughout the work.

The quality of the conversion may have a significant influence on the simulation results, since in the devices irradiated with a proton beam, the fraction of energy allocated to the generated neutrons and gamma rays is significant in the particle transport calculations, and it depends on the geometry of the device components and the chemical composition of the material. To solve these and many other problems, the milestone of successfully

converting a CAD model to a high-detail MCNP model was implemented. To achieve this goal, the McCAD software package was used, resulting in a 3D LIEBE target model suitable for further use in the Monte-Carlo-based MCNP software package.

4. Simulation of the LIEBE Target

Monte Carlo methods are used to solve any system with stochastic properties with realistic objects. Since there is uncertainty in the entire nuclear particle transport problem, it can be said that the movement of particles in a certain space has stochastic properties. This method is able to simulate physical experiments, with only a few restrictions on the geometrical conditions, and its results are more accurate than those of the deterministic method. Deterministic methods can quickly obtain an approximate solution to the transport equation by discretizing direction, energy, space, and time. Systems of nuclear objects are characterized by complex geometry, complex energy spectrum and anisotropic scattering. The Monte Carlo method is often used specifically for nuclear facilities. When the Monte Carlo method is applied to the simulation of particle transport, first, a random movement of a single particle in a known environment is performed, and then random experimental values are obtained by observing the number of particle histories. Finally, an estimate of the numerical characteristics of the random variable is obtained. The Monte Carlo method involves three processes in solving the neutron transport equations: (1) the source is determined using a probability distribution; (2) tracking the particle's local energy and direction; (3) data recording and analysis of results.

Particle transport calculations were performed using the 3D Monte Carlo code MCNP, which is widely used in nuclear applications for neutron particle transport calculations, together with various nuclear reaction cross-section libraries and geometry models.

The modified model was converted to the MCNP input, as outlined in Section 3. A 1 mm radii, mono-energetic 70 MeV—100 μA or 1.987742×10^{16} #/cm^2/s flux proton beam falling on the liquid lead target LIEBE was modeled. FENDL-3.1 cross-section data library was used, and dose rate maps of 10^9 particle histories were calculated, from which proton-, neutron- and gamma-induced dose rate maps and fluxes were calculated.

Nuclear reactions such as ^{208}Pb(p,n) or ^{208}Pb(p,γ) have cross sections exceeding 10 barns (see Figure 10 for more information), so the reaction produces a broad spectrum of neutrons and gamma rays. Therefore, to evaluate the radiation processes in the target and the surrounding premises, it is necessary to determine the possible proton-initiated neutron and gamma-ray fluxes.
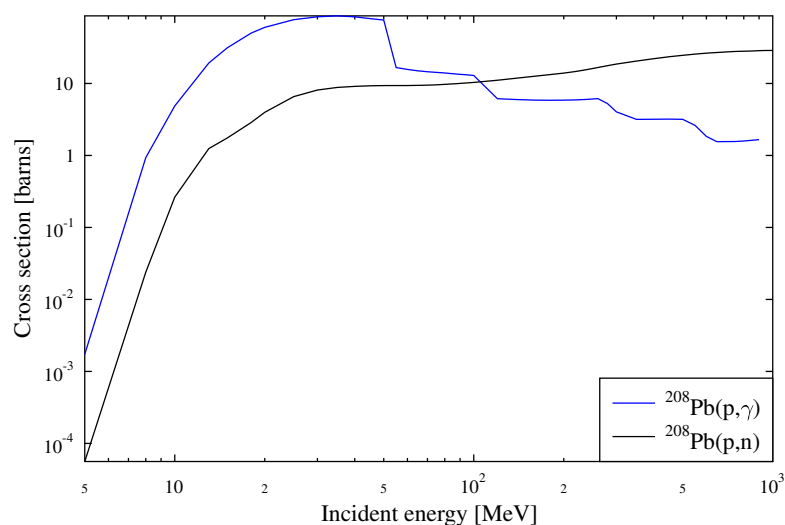

Figure 10. Lead isotope ^{208}Pb(p,n) and ^{208}Pb(p,gamma) reaction cross sections [14].

Simulation results of proton scattering allow us to predict the possible distribution of flux during direct interaction of the beam with the lead target (see Figure 11). Figure 12,

presenting the proton beam penetration depth inside the target, shows that the target effectively absorbs the proton beam, with the maximum flux reaching 1.885490×10^{16} #/cm^2/s which is close to the flux of the proton beam: 1.987742×10^{16} #/cm^2/s. Additionally, the proton beam penetrates roughly 7 mm inside the target. Consequently, it can be seen that very little scattering of the proton beam occurs before the beam hits the LBE inside the irradiation chamber. It should also be noted that the difference between the maximum flux values of Figures 11 and 12 is due to the fact that the tally mesh in Figure 11 is more coercive than that of Figure 12, so the mean value at a single cell is lower in Figure 11 than in Figure 12.
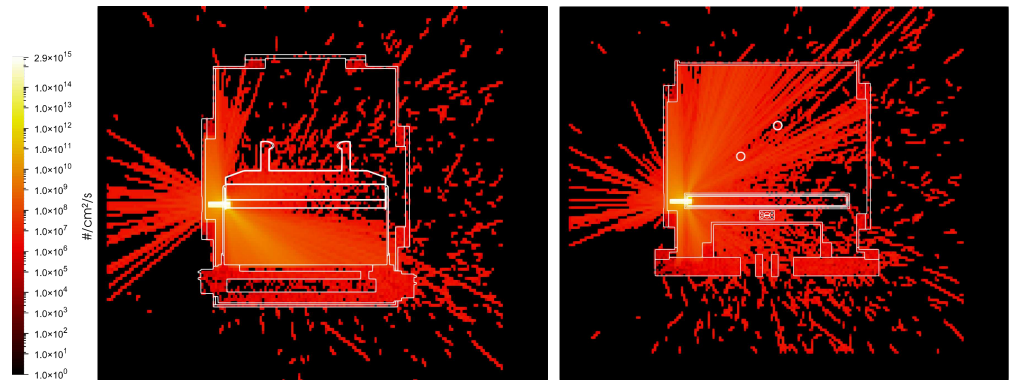
Figure 11. Proton-induced flux [#/cm^2/s] map cross sections from the side (left) and top (right) of the target along the proton beam.

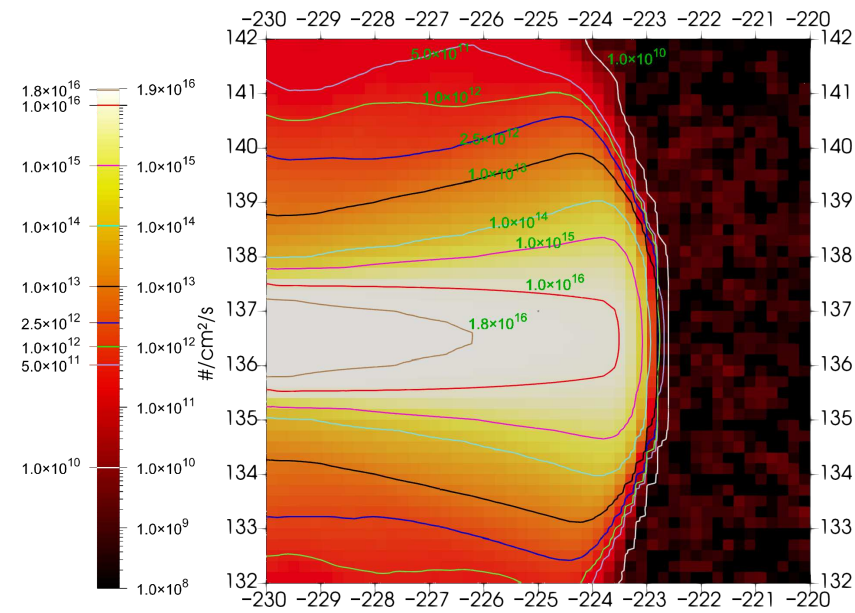**Figure 12.** Proton flux [#/cm^2/s] xy plane cross-section along the proton beam path of the proton beam penetration depth inside the LBE (coordinates are in [mm]).

The highest proton dose is contained to the beam location (Figure 13) until the target is reached. Most of the proton dose is absorbed inside, with practically no dose present outside the LIEBE target.
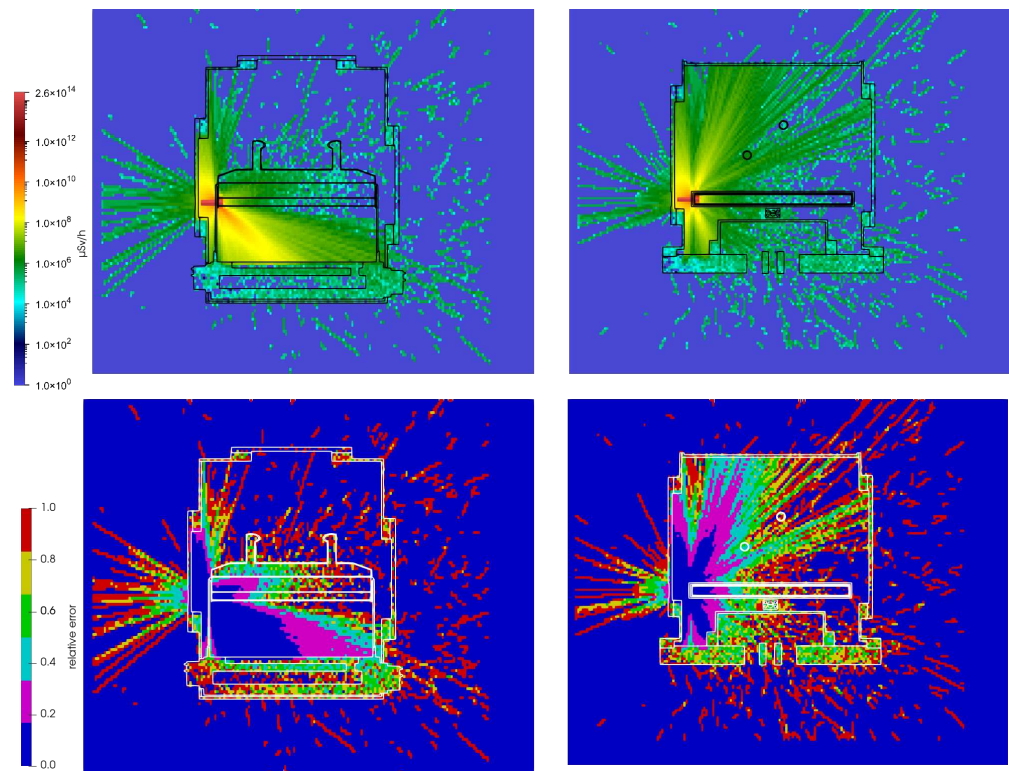
Figure 13. Proton-induced dose rate map (top) [µSv/h] and relative error (bottom) cross sections along the beam path in the LIEBE target.

Monte Carlo calculations made it possible to determine the distributions of neutrons and gamma fluxes in and around the LIEBE target. The error of the calculation results reaches a maximum error of 15% in the places farthest from the source, and the results are presented in Figure 14 (neutrons) and Figure 15 (gamma).
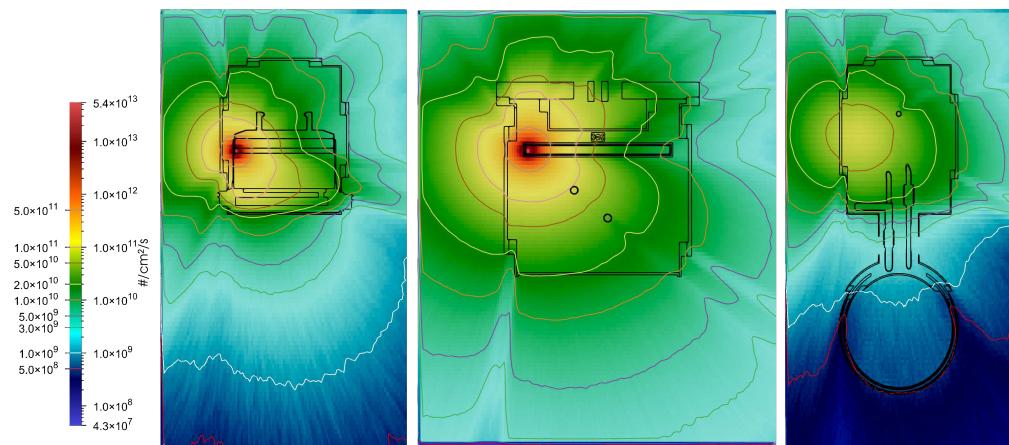

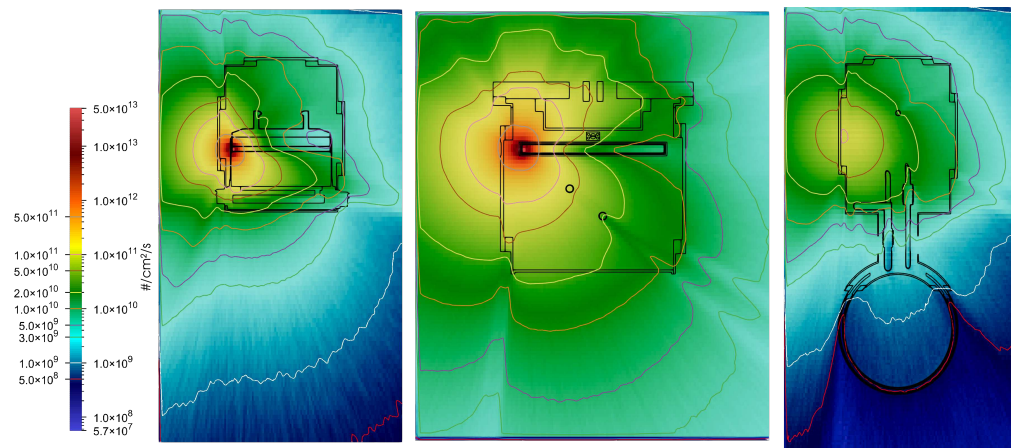**Figure 14.** Distribution of neutron flux in the LIEBE target, [#/cm^2/s].

Figure 15. Distribution gamma flux in the LIEBE target, [#/cm^2/s].

Gamma and neutron dose rate maps (see Figure 16 top) present a picture in correspondence with the proton flux results. Since the proton beam effectively interacts with the target, the location at around the target edge is where the highest dose rates of neutrons and gamma rays are generated. Gamma and neutron dose rates there reach almost 2 MSv/h each. However, around the target dose rates are much lower: around 361 Sv/h for gamma rays and 214 Sv/h for neutrons (Table 1). The error of the dose rate calculation results (Figure 16 bottom left and right) reaches a maximum error of 22% farthest away from the source.
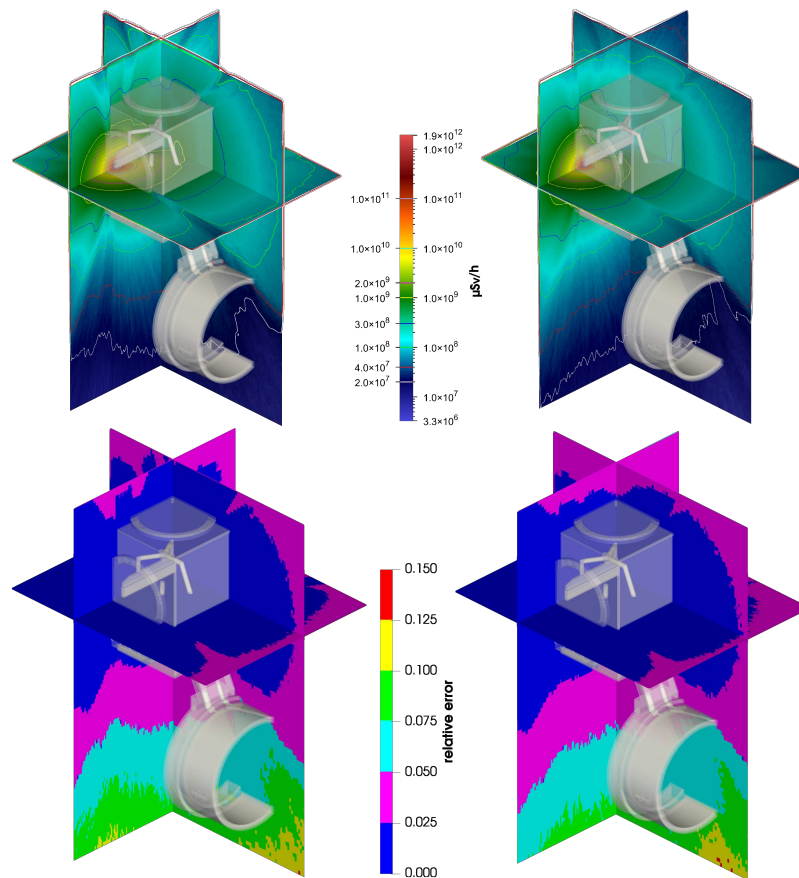

Figure 16. Neutron (top left) and gamma (top right)-induced dose rate map [μSv/h] and neutron (bottom left) and gamma (bottom right) relative error cross sections in the LIEBE target.

Table 1. Comparison of main obtained indicators.

	Neutrons	**Gamma**
Highest local dose rate	1.9 MSv/h	1.9 MSv/h
Highest dose rates around the target	361 Sv/h	214 Sv/h
Highest relative dose rate error	22%	22%

Figure 17 presents gamma and neutron dose rates and their ratio, as well as the relative error along the path of the beam. The dose rate is highest at the beam entrance to the target; their interaction with the material is most intense. Before the target ratio of gamma and neutron doses is close to one, however, the LBE inside the irradiation chamber ratio falls significantly due to more effective gamma-ray absorption. Outside the irradiation chamber ratio again reaches values close to 1. The slight bump on the left in Figure 17, which roughly begins at 200 mm, is due to an increased dose rate of neutrons and gamma at the other edge of the irradiation chamber when protons interact with stainless steel.
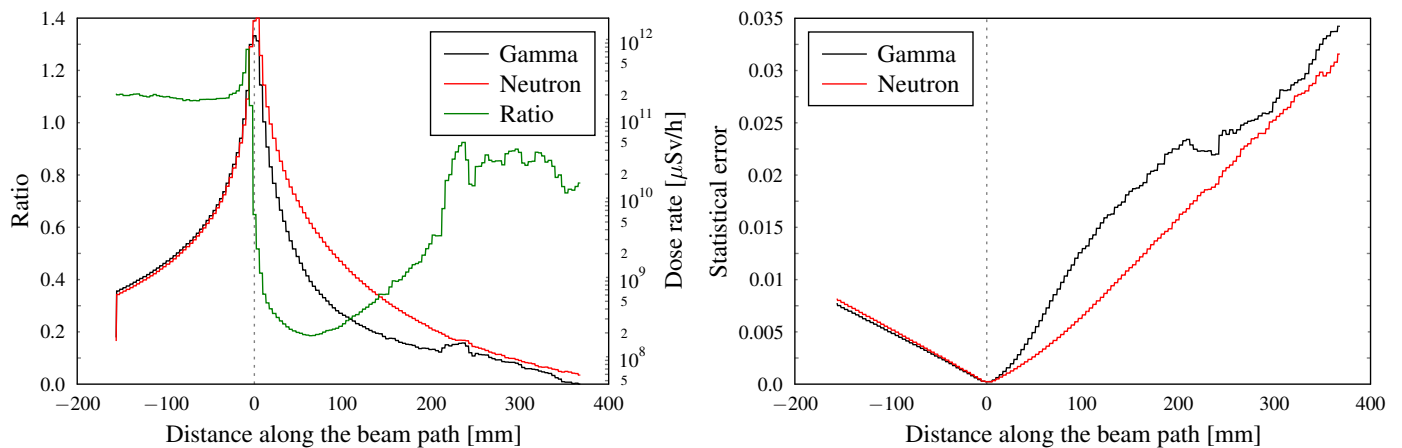

Figure 17. Gamma and neutron dose rates and their ratio (left) and the relative error along the beam path (right) (0 mm—irradiation chamber edge).

5. Conclusions

This paper presented an MCNP simulation of a 70 MeV proton beam and LIEBE target interaction. LIEBE is a prototype liquid metal ion beam target aimed at solving issues of accommodating a high-power beam and ensuring adequate extraction of short-lived radioisotopes. For the simulation, a detailed model of the LIEBE target was developed based on the CAD drawings through a process involving manual decomposition and automated conversion with the help of the SALOME software McCAD module.

The proton flux distribution after the beam impact on the target was obtained from the simulations. The 70 MeV–100 μA proton beam penetrated roughly 7 mm deep into the liquid LBE and produced neutrons and gamma rays during the interaction with the material. Most of the proton dose was absorbed inside the target.

The simulations provided the dose rate distributions of neutron and gamma radiation around the LIEBE target. The maximum obtained dose around the target was roughly 361 Sv/h for gamma rays and 214 Sv/h for neutrons.

To obtain additional data and perform a comparative study in future work using the MCNP code, we plan to perform more accurate estimates of radiation processes (material activation, heat of decay or dose rate) by modeling thick lanthanum targets at high nuclear spallation energies.

References

1. Popescu, L.; Houngbo, D.; Dierckx, M. High-power target development for the next-generation ISOL facilities. *Nucl. Instrum. Methods Phys. Res. Sect. B* **2020**, *463*, 262–268. [CrossRef]
2. Pamies, F.B.; Stora, T.; Barbero, E.; Barozier, V.; Bernardes, A.; Catherall, R.; Fernandez, B.C.; Crepieux, B.; Delonca, M.; Dierckx, M.; et al. The LIEBE high-power target: Offline commissioning results and prospects for the production of 100Sn ISOL beams at HIE-ISOLDE. *Nucl. Instrum. Methods Phys. Res. Sect. B* **2020**, *463*, 128–133. [CrossRef]
3. Delonca, M. Development of New Target Concepts for Proton Beams at CERN/ISOLDE. Ph.D. thesis, Universite de Technologie, Belfort, Montbeliard, France, December 2015.
4. Houngbo, D.; Bernardes, A.; David, J.; Delonca, M.; Kravalis, K.; Lahiri, S.; Losito, R.; Maglioni, C.; Marchix, A.; Mendonça, T.; et al. Development of a liquid Pb-Bi target for high-power ISOL facilities. *Nucl. Instrum. Methods Phys. Res. Sect. B* **2016**, *376*, 57–59. [CrossRef]
5. Werner, C.J. *MCNP Users Manual-Code Version 6.2 (No. LA-UR-17-29981)*; Los Alamos National Laboratory: Los Alamos, NM, USA, 2017.
6. Yican, W. *Fusion Neutronics*; Springer Nature Singapore: Singapore, 2017. [CrossRef]
7. Shultis, J.K.; Faw, R.E. *An MCNP Primer*; Kansas State University: Manhattan, KS, USA, 2011.
8. Booth, T. *Sample Problem for Variance Reduction in MCNP (No. LA-10363-MS)*; Los Alamos National Laboratory: Los Alamos, NM, USA, 1985.
9. Hernandez-Davila, V.M.; Soto-Bernal, T.G.; Vega-Carrillo, H.R. Determination of neutron fluence-to-dose conversion coefficients by means of artificial neural networks. *Appl. Radiat. Isotopes* **2013**, *83*, 249–251. [CrossRef]
10. Ribes, A.; Caremoli, C. SALOME platform component model for numerical simulation. In Proceeding of the 31st Annual International Computer Software and Applications Conference, Beijing, China, 24–27 July 2007.
11. Lu, L.; Fischer, U.; Pereslavtsev, P. Improved algorithms and advanced features of the CAD to MC conversion tool McCad. *Fusion Eng. Des.* **2014**, *89*, 1885–1888. [CrossRef]
12. Brun, E.; Damian, F.; Diop, C.; Dumonteil, E.; Hugot, F.; Jouanne, C.; Lee, Y.; Malvagi, F.; Mazzolo, A.; Petit, O.; et al. TRIPOLI-4®, CEA, EDF and AREVA reference Monte Carlo code. *Ann. Nucl. Energy* **2015**, *82*, 151–160. [CrossRef]
13. Agostinelli, S.; Allison, J.; Amako, K.; Apostolakis, J.; Araujo, H.; Arce, P.; Asai, M.; Axen, D.; Banerjee, S.; Barrand, G.; et al. GEANT4—A simulation toolkit. *Nucl. Instrum. Methods Phys. Res. Sect. A* **2003**, *506*, 250–303. [CrossRef]
14. Brown, D.A.; Chadwick, M.B.; Capote, R.; Kahler, A.C.; Trkov, A.; Herman, M.W.; Sonzognia, A.A.; Danond, Y.; Carlsone, A.D.; Dunnf, M.; et al. ENDF/B-VIII.0: The 8th Major Release of the Nuclear Reaction Data Library with CIELO-project Cross Sections. *New Stand. Therm. Scatt. Data Nucl. Data Sheets* **2018**, *148*, 1–142. [CrossRef]